# Computer modeling of water and salt transport in RO membrane active layers

Jed W. Pitera, Young-hye Na, Ankit Vora, Geraud Dubois

IBM Research, Science & Technology
IBM Almaden Research Center, 650 Harry Road, San Jose CA 95120
pitera@us.ibm.com

## ABSTRACT

As part of a combined computational and experimental effort to develop new reverse osmosis desalination membrane materials, we have carried out detailed equilibrium and nonequilibrium molecular dynamics simulations of the aromatic polyamide active layers of reverse osmosis desalination membranes. Simulations carried out at low salt concentration yield hydraulic permeabilities in good agreement with experimental results for both traditional and novel membrane materials. The pressure and concentration profiles observed in nonequilibrium simulations support a solution-diffusion mechanism for water transport, even at the nanoscale. In the case of salt transport, our simulations reveal the critical role of charged groups in altering the uptake and diffusion of ions in the polymer. These results illustrate the emerging power of detailed computer simulations in the development of new materials.

***Keywords***: desalination, reverse osmosis, membrane, simulation

## 1 INTRODUCTION

Modern reverse osmosis (RO) desalination membranes are composite membranes consisting of a thin (~100 nm) aromatic polyamide active layer atop a thicker porous polysulfone layer which is itself supported by a woven mechanical support layer. The active layer is responsible for the remarkable ability of these membranes to block the transport of salt ions while allowing rapid permeation by water molecules [1]. The active layer is dense, highly crosslinked [2], yet can have significant water content [3]. It is formed in situ by interfacial polymerization and is difficult to separate from the polysulfone support, making physical measurements difficult. In addition, NMR experiments have detected the presence of up to 0.5 M of NaCl in the active layer [4]. Given these physical measurements, there is intense interest in the microscopic details of water and salt transport through the active layer. Previous attempts to simulate a traditional meta-phenylenediamine (MPD)/trimesoyl chloride (TMC) active layer [5,6] yielded water permeabilities comparable to experiment, and predicted that salt rejection arises from an almost complete exclusion of $Cl^-$ from the membrane, rather than the mix of exclusion and diffusion observed experimentally [7].

## 2 METHODS

In the present work we carried out computer simulations of two different RO membrane active layers, one based on a traditional MPD/TMC chemistry and another based on a hexafluoroalcohol-containing diamine HFA-MDA/TMC. The latter "i-phobe 1" membrane was developed in the experimental part of this research program [8].

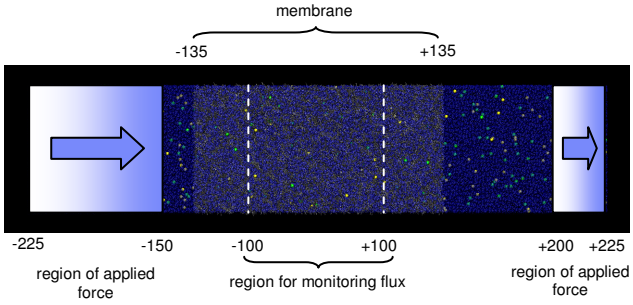


Figure 1: Image of the typical simulation geometry. All distances are in Angstrom (Å.). The long z axis of the simulation cell is approximately 450 Å, and the short x and y axes are each 100 Å . The membrane occupies the central region of the simulation cell from -135 to 135 Å . The shaded blue region and arrows denote the region of applied force for non-equilibrium calculations.

### 2.1 Membrane preparation

Model membrane topologies were constructed by directly simulating the process of interfacial polymerization. Mixtures of coarse-grained models of the trimesoyl chloride and m-phenylene diamine (for traditional RO) or HFA-MDA (for i-phobe 1 RO) membrane precursors were prepared. The LAMMPS simulation package [9] was then used to carry out a reactive Langevin dynamics simulation. During the simulation, any time unreacted acid chloride and amine groups were in van der Waals contact, an amide cross-link was formed between the two groups. This process was continued until no more cross-links could be formed.

The resulting crosslink graph was examined to find the largest connected subgraph, corresponding to the main membrane macromolecule. The coordinates of this subgraph were then used in a back-mapping process to construct a corresponding atomistic model of the membrane

suitable for molecular dynamics simulation. Permeant waters and ions were then randomly placed around the membrane to construct a rectangular simulation cell with the membrane at its center and the membrane normal aligned along the z axis.

## 2.2 Molecular model

After membrane preparation, all subsequent simulations used an all-atom representation of the membrane and permeants. The membrane materials were modeled using the GAFF force field [10] with AM1-BCC [11] atomic partial charges. The TIP3P water model [12] was used in conjunction with $Na^+$ and $Cl^-$ parameters optimized for that model [13]. Non-bonded interactions were smoothly truncated between 0.8 and 1 nm, and the particle-particle particle-mesh Ewald technique was used to treat long-range electrostatic interactions [14]. All simulations were carried out using the LAMMPS simulation package [9] on an IBM BlueGene/L supercomputer [15].

## 2.3 Equilibrium simulation

After preparation of the the atomistic models and energy minimizations to remove unfavorable contacts, the volume of each system was equilibrated by extensive (>10 ns) NPT simulations at 300 K and 1 atm pressure. Table 1 lists some summary statistics of the membrane systems after this equilibration phase. After equilibration, microcanonical (NVE) simulations were used to determine the equilibrium diffusion coefficients for water within the membrane.

| | MPD/TMC | HFA-MDA/TMC | | |
|---|---|---|---|---|
| NaCl (ppm) | 2300 | 1800 | 35000 | 35000 |
| pH | 7.0 | 7.0 | 7.0 | 12.0 |
| z (Å ) | 440 | 464 | 565 | 560 |
| x, y (Å ) | 100 | 100 | 101 | 100 |
| atoms | 404521 | 441595 | 536267 | 535553 |
| Membrane and solute density ($g/cm^3$) | 1.28 | 1.38 | 1.32 | 1.4 |

Table 1: Composition and dimensions of equilibrated RO membrane systems.

## 2.4 Non-equilibrium simulation

The applied force technique [16] was used to create a pressure differential across the equilibrated membranes. The permeant distant from the membrane was subjected to a constant force acting along the +z direction. This produces a pressure differential across the membrane, and the corresponding chemical potential difference results in the movement of water across the membrane. Harmonic restraints were applied to the membrane atoms to prevent compaction or translation due to the applied pressure. Nonequilibrium simulations were carried out at several different applied pressures and the water flux across the central membrane region was recorded. The pressure differential can be determined from

$$\Delta P = nf / A \tag{1}$$

Where $n$ is the number of permeants subjected to the constant force $f$ and $A$ is the cross-sectional area of the membrane. The hydraulic permeability $L_p$ can be computed from the flux and pressure differential by:

$$L_P = \frac{j_n}{\Delta P} \frac{V_W}{N_a A} \tag{2}$$

Where $j_n$ is the number flux of water molecules, $V_w$ the molar volume of water, $N_a$ Avogadro's number, and $A$ the cross-sectional area of the membrane. Non-equilibrium simulations were carried out at multiple applied pressures ranging from 100-1700 bar (1450-24650 psi).

# 3 RESULTS

## 3.1 Water permeability

The water permeabilities of MPD/TMC and HFA-MDA/TMC membrane models calculated from both equilbirium and non-equilibrium simulations are reported in table 2. The experimental values reported are the typical ranges of permeabilities for dense sea water RO MPD/TMC and HFA-MDA/TMC results from [7] and [8], respectively.

| | MPD/TMC | HFA-MDA/TMC |
|---|---|---|
| **Equilibrium** | | |
| $K_w$ | 0.34 | 0.41 |
| $D_w$ ($m^2/s$) | $0.11 \times 10^{-8}$ | $0.22 \times 10^{-8}$ |
| $L_p$ ($m^2$ hr bar) | 0.48 | 1.16 |
| **Non-equilibrium** | | |
| $L_p$ ($m^2$ hr bar) | 0.9 ± 0.5 | 1.8 ± 0.6 |
| **Experiment** | | |
| $L_p$ ($m^2$ hr bar) | 0.3-0.8 | 1.1-1.6 |

Table 2: Hydraulic permeabilities for MPD/TMC and HFA-MDA/TMC membrane models calculated from equilibrium and non-equilibrium simulations.

## 3.2 pH-dependent changes in HFA-MDA/TMC

Figure 2 shows the density of membrane, water and salt atoms in HFA-MDA/TMC membranes simulated at high salt (35000 ppm NaCl) and with ionization states corresponding to pH 7 (all hexafluoroalcohol groups protonated) and pH 12 (all hexafluoroalcohol groups

ionized). The large number of negatively charged groups at pH 12 cause the membrane to swell by approximately 8 %, and draw positively charged $Na^+$ ions into the membrane to balance the negative charge. The swelling increases the water content of the membrane from 0.41 g/cm$^3$ to 0.45 g/cm$^3$. The increased water content of the membrane at high pH is a partial explanation for the experimentally observed 1.5-fold increase in water permeability of HFA-MDA/TMC membranes with increasing pH [8].

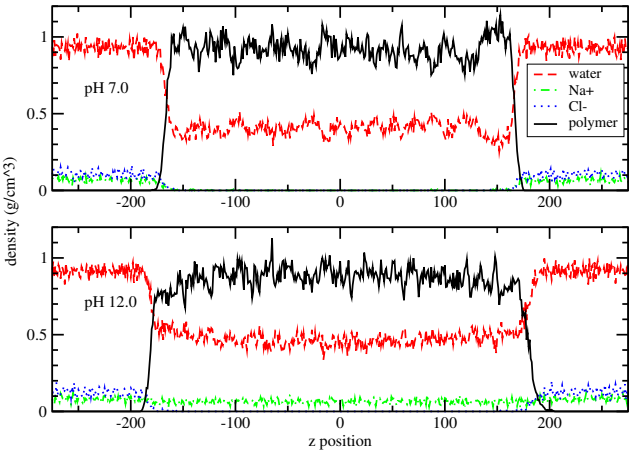


Figure 2: Density (in g/cm$^3$) of different components of the HFA-MDA/TMC membrane as a function of position along the z axis.

## 3.3 Pressure and concentration profile

Figure 3 shows the pressure and concentration profiles across an RO membrane active layer as predicted by the solution-diffusion model [16] and determined from a nonequilibrium simulation of MPD/TMC at an applied pressure of 375 bar. There is good qualitative agreement between the solution-diffusion model and the simulation results. The pressure is roughly constant at the feed pressure across the membrane and drops to the flow pressure at the back face of the membrane. Similarly, the water concentration in the membrane is linear, as expected from Fickian diffusion.

# 4 CONCLUSIONS

Large-scale detailed atomistic simulations of RO active layer polyamides are now a useful tool for designing new membrane materials. Simulations offer a detailed, microscopic picture of the structure of the active layer as well as the transport of water and salt. Equilbirium and non-equilibrium methods can both be used to determine hydraulic permeabilities with good quantitative agreement

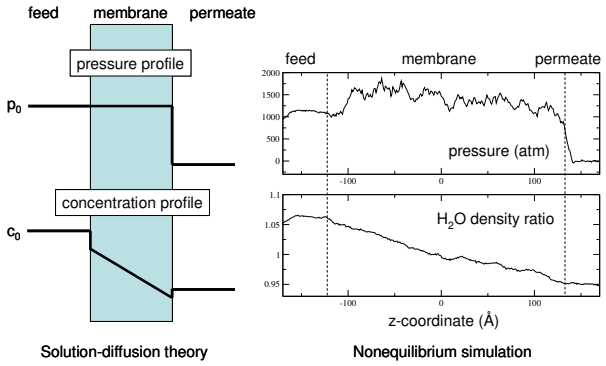


Figure 3: Comparison of pressure (top) and water concentration (bottom) profiles in a reverse osmosis desalination membrane predicted by solution-diffusion theory (left) and observed in nonequilibrium atomistic simulations (right).with experiment.

Furthermore, the simulations can capture the effect of chemical changes on water permeability. Simulations of HFA-MDA/TMC membranes at pH 7 and 12 show that the membrane swells at high pH, allowing the entry of more water molecules and $Na^+$ ions, but continuing to exclude larger $Cl^-$ ions. This swelling may be the origin of the experimentally observed increase in flux through HFA-MDA/TMC membranes at high pH. Finally, the microscopic view of water permeation provided by simulations also allows us to compare the observed results with the macroscopic solution-diffusion theory of permeation. The pressure and concentration profiles observed from non-equilibrium simulations are qualitatively consistent with the solution-diffusion model, validating the long-held belief that RO obeys such a mechanism. With these results, it is clear that large-scale supercomputing, long a valuable tool for scientific exploration, has potential use in the design of new RO active layer materials with improved performance.

# REFERENCES


[1] A.C. Sagle and B.D. Freeman, "Fundamentals of Membranes for Water Treatment", Texas Water Development Board Numbered Reports, R363, 2004.

[2] X. Zhang, D.G. Cahill, O. Coronell and B.J. Marinas, J. Mem. Sci., 331, 143-151, 2009.

[3] O. Coronell, M.I. Gonzalez, B.J. Marinas and D.G. Cahill, Environ. Sci. Technol., 44, 6808-6814, 2010.

[4] X. Xu and R.J. Kirkpatrick, J. Mem. Sci., 280, 226-233, 2006.

[5] Z.E. Hughes and J.D. Gale, J. Mater. Chem., 20, 7788-7799, 2010.

[6] Y. Luo, E. Harder, R.S. Faibish and B. Roux, J. Mem. Sci., 384, 1-9, 2011.

[7] G.M. Geise, H.B. Park, A.C. Sagle, B.D. Freeman and J.E. McGrath, J. Mem. Sci., 369, 130-138, 2011.
[8] Y.H. La, R. Sooriyakumaran, D.C. Miller, M. Fujiwara, Y. Terui, K. Yamanaka, B.D. McCloskey, B.D. Freeman and R.D. Allen, J. Mater. Chem, 20, 4615-4620, 2010.
[9] S.J. Plimpton, J. Comp. Phys., 117, 1-19, 1995.
[10] J. Wang, R.M. Wolf, J.W. Caldwell, P.A. Kollman and D.A. Case, J. Comp. Chem, 25(9), 1157-1174, 2004.
[11] A. Jakalian, B.L. Bush, D.B. Jack, C.I. Bayly, J. Comp. Chem., 21(2), 132-146, 2000.
[12] W.L. Jorgensen, J. Chandrasekhar, J.D. Madura, R.W. Impey and M.L. Klein, J. Chem. Phys., 79(2), 926-935, 1983.
[13] I.S. Joung and T.E. Cheatham, J. Phys. Chem. B, 112(30), 9020-9041, 2008.
[14] S.J. Plimpton, R. Pollock and M. Stevens, Proc. Of the 8th SIAM Conf. on Parallel Processing for Scientific Computing, 1997
[15] F. Allen et al, IBM Syst. J., 40(2), 310-327, 2001.
[16] F. Zhu, E. Tajkhorshid and K. Schulten, Phys. Rev. Lett., 93, 224501, 2004.
[17] J. Wijmans and R.W. Baker, J. Mem. Sci., 107, 1-21, 1995.